



Published in final edited form as:

Nat Struct Mol Biol. 2010 January ; 17(1): 77–82. doi:10.1038/nsmb.1728.

Catalysis of the microtubule on-rate is the major parameter regulating the depolymerase activity of MCAK

Jeremy R. Cooper¹, Michael Wagenbach¹, Charles L. Asbury¹, and Linda Wordeman¹

¹Dept. of Physiology and Biophysics, University of Washington School of Medicine, Seattle, WA 98195 USA

Abstract

The kinesin-13, MCAK, is a critical regulator of microtubule dynamics in eukaryotic cells¹. We have functionally dissected the structural features responsible for MCAK's potent microtubule depolymerization activity. MCAK's positively charged neck enhances its delivery to microtubule ends, not by tethering the molecule to microtubules during diffusion, as commonly thought, but by catalyzing the association of MCAK to microtubules. On the other hand, this same positively charged neck slightly diminishes MCAK's ability to remove tubulin subunits once at the microtubule end. Conversely, dimerization reduces MCAK delivery but improves MCAK's ability to remove tubulin subunits. The reported kinetics for these events predict a non-specific binding mechanism that may represent a paradigm for the diffusive interaction of many microtubule binding proteins.

INTRODUCTION

The kinesin-13 protein MCAK (Mitotic Centromere Associated Kinesin) can both rapidly depolymerize microtubules^{2,3}, and also provide its own means of transportation to microtubule ends where the action of depolymerization takes place⁴. This is especially beneficial in living cells where microtubule ends may be relatively sparse compared to microtubule lattice and are predominantly located at the cell periphery. Here for the first time we precisely quantify the relative functional benefits of two important structural features of MCAK, which are common features of microtubule motors: dimerization and the positively charged neck. We show that features that improve one function may impede another.

The MCAK neck is an α -helical ~60 amino acid region located adjacent to the kinesin motor domain^{5,6}. A high concentration of lysine and arginine residues confers a charge of about +5 on the neck at neutral pH. The positive charges in the neck are essential for MCAK to depolymerize microtubules under physiological conditions⁵, however, the mechanistic role of this structural element is entirely unknown. Hypotheses have been proposed envisioning

Users may view, print, copy, and download text and data-mine the content in such documents, for the purposes of academic research, subject always to the full Conditions of use:http://www.nature.com/authors/editorial_policies/license.html#terms

Corresponding Author: Linda G. Wordeman, Department of Physiology & Biophysics, Box 357270, University of Washington School of Medicine, Seattle, WA 98195, worde@u.washington.edu, Phone:206-543-4135, Fax: 206-685-0619.

Supplementary Information is linked to the online version of the paper.

the neck in various roles including (i) a loose tether that allows the molecule to diffuse along the microtubule lattice^{4,5,6}, (ii) an obstructive element that prevents tight binding to the lattice⁶, (iii) a pry bar that destabilizes lateral interactions at the microtubule end⁶, and (iv) a facilitator of cross-linking between protofilament peels at the depolymerizing ends of microtubules⁷.

We used total internal reflection fluorescence (TIRF) microscopy with recombinant mammalian GFP-MCAK (*Cricetulus griseus*) to precisely define the contribution of the positively charged neck to MCAK's microtubule depolymerization activity at the single molecule level. We show that neither the neck nor the quaternary structure of the molecule has any significant influence on diffusion of the motor along the microtubule lattice once bound. Instead, the neck activates MCAK by increasing the flux of motors to the microtubule end. It does this by increasing the association rate of the motor to microtubules by two orders of magnitude. By influencing the on-rate and off-rate in parallel, the neck lowers the energy barrier for association with microtubule lattice to enable the molecules to engage in 1D diffusion. In contrast, the diffusion coefficient is a relatively constant parameter for MCAK constructs that vary widely in size, structure and activity. Therefore, it is the association and dissociation rates that biological systems evolutionarily refine and functionally regulate to modulate cellular activities.

Our data show that it is the on-rate catalyzed by the neck, rather than the diffusion constant, which is similar to other measured microtubule diffusers, that is the single most important parameter controlling the depolymerase activity of MCAK. Surprisingly, this important feature is utilized at the expense of efficacious tubulin dimer removal and underscores the compromises that arise during molecular evolution.

RESULTS

To investigate the role of MCAK's positively charged neck, we expressed and purified both full-length wild-type MCAK protein MCAK(FL), ("full length", Fig. 1A), and a mutant protein MCAK(FL-NN), ("full length, neutralized neck", Fig. 1A) in which 10 of the positively charged lysine and arginine residues in the neck region were mutated to neutral alanine residues. We used a real-time microscopic assay to compare the depolymerization efficacy of EGFP-MCAK(FL) and EGFP-MCAK(FL-NN). In this assay, Cy5-labeled microtubules, stabilized with the non-hydrolyzable GTP analogue, GMPCPP, were tethered to a PEG-passivated coverslip⁸. The ends of the microtubules were tracked throughout time to provide a measure of depolymerization that encompasses the combined shortening rates of both microtubule ends. This was repeated over a range of MCAK concentrations to obtain a dose-response relationship (Fig. 1B and 1C). At low MCAK concentrations (well below saturation), we found that the dependency of the depolymerization rate upon concentration approaches a linear relationship (Fig. 1C). The catalytic efficiency, k_b , which defines this relationship, is the slope of the asymptote line of a Michaelis-Menten fit to the data (Fig. 1C). Specifically, k_b is determined as $V_{\max}/K_{1/2}$, where V_{\max} and $K_{1/2}$ are the classical Michaelis-Menten parameters (table S1). The parameter k_b provides a lucid measure of the overall depolymerization efficacy since it linearly relates depolymerization rate to concentration. Compared to MCAK(FL), the mutant MCAK(FL-NN) exhibits a 45-fold

reduction in k_b ($0.116 \mu\text{m} \cdot \text{min}^{-1} \cdot \text{nM}^{-1}$ vs. $0.0026 \mu\text{m} \cdot \text{min}^{-1} \cdot \text{nM}^{-1}$, Table 1). Thus, consistent with *in vivo* data⁵, neutralizing the positive charges in the neck severely cripples MCAK's ability to depolymerize microtubules.

Neck neutralization inhibits microtubule binding but not diffusion

To determine which parameters of MCAK's activity are affected by its positively charged neck we used Total Internal Reflection Fluorescence (TIRF) microscopy to image single GFP labeled MCAK(FL) and MCAK(FL-NN) molecules as they bound to the microtubule lattice, diffused 1-dimensionally along the lattice, and then dissociated. We then compared the binding kinetics and 1-dimensional diffusion of wild-type MCAK (FL) to the neutralized neck mutant MCAK(FL-NN) (Fig. 2). Diffusion coefficients (Table 1) were calculated from plots of mean square displacement versus time (Fig. 2B). Association and dissociation rates of binding to the microtubule lattice were calculated from the distributions of dwell times (Fig. 2C, see analysis section in full methods). Finally, using these measurements of association rate (k_{ON}), dissociation rate (k_{OFF}), and diffusion coefficient (D), we calculated the flux per concentration (J_0/C_m) of MCAK arriving at each microtubule end via lattice diffusion according to the following equation (derived from⁴):

$$\frac{J_0}{C_m} = \left(\frac{D}{k_{\text{off}}} \right)^{1/2} \cdot k_{\text{on}}$$

From these data (Table 1), we find that MCAK(FL-NN) exhibits an enormous 170-fold reduction in lattice association rates compared to the wild-type MCAK(FL). More importantly, this difference in lattice association rate leads to a similar 140-fold reduction in MCAK(FL-NN) flux to microtubule ends. Thus, the positively charged neck is critical for MCAK delivery to microtubule ends, specifically by facilitating the initial step of binding to the microtubule lattice. The differences in diffusion coefficient and dissociation rate are much slighter (Table 1). These parameters, therefore, are negligible with respect to the reduced delivery of MCAK(FL-NN) to microtubule ends. These data precisely define and quantify the mechanism by which the neck domain converts the inert motor domain of MCAK into an efficient depolymerizer at physiological ionic strength.

It is also important to note that the dissociation rate of MCAK(FL-NN) is reduced compared to wild-type MCAK(FL), corresponding to a longer dwell time for the neutralized neck mutant. This surprising finding demonstrates that MCAK(FL-NN) molecules that are able to bind to the lattice have no trouble hanging on, clearly disproving a long favored hypothesis that the positively charged neck acts as a tether for holding the MCAK molecule on the microtubule lattice^{4,5,6}.

Neck neutralization facilitates tubulin removal

We then asked whether the positively charged neck might also play a role in MCAK's ability to depolymerize microtubules after arrival at the microtubule end as previously proposed^{6,7}. To answer this question, we calculated the average number of tubulin subunits that are removed for each MCAK end-binding event (which we refer to as the "removal

factor”) for both MCAK(FL) and the mutant MCAK(FL-NN). The removal factor is calculated by dividing k_b (with units converted to express the depolymerization rate as the number of tubulin subunits removed from each microtubule end per second, see analysis section in full methods) by the flux of MCAK to each microtubule end, J_0/C_m . Surprisingly, we found that MCAK(FL-NN) on average removes more than 3-times the number of tubulin subunits per end binding event than the wild type MCAK(FL) (58 vs. 18 tubulin subunits removed, Table 1). This indicates that the positively charged neck significantly, and surprisingly, impedes MCAK’s ability to remove tubulin subunits from the microtubule end. If the removal factor is an indirect measure of processivity then we speculate that the reduced dissociation rate enhances the processivity of MCAK motors. This would be the first demonstration that removing positive charges on the neck domain enhanced processivity and represents a mechanistic specialization of depolymerizing kinesins. For motile kinesins, the addition of positive charges generally leads to an increase in processivity⁹. Despite the detrimental effect of reduced processivity, the benefit that the positively charged neck provides in terms of delivery of MCAK to the microtubule end affords the wild-type MCAK(FL) a general advantage over MCAK(FL-NN) as quantified by k_b . Thus, the benefit of the positively charged neck, with regard to increasing the association rate of MCAK to microtubules, outweighs the disadvantage it imparts in slightly impeding the removal of tubulin subunits.

Dimerization inhibits microtubule binding

We similarly characterized the contribution of MCAK’s native homodimeric quaternary structure. MCAK’s ability to dimerize depends on both the N-terminal and C-terminal domains of the protein¹⁰. The specific role of dimerization is not well understood due to the fact that monomeric mutants containing only the neck and motor (i.e. missing the N-terminus and C-terminus dimerization domains) depolymerize quite well^{5,10,11}. A recent study suggests that monomeric MCAK may have a more difficult time disengaging from detached tubulin subunits than full-length dimeric MCAK¹². Thus, dimerization has been hypothesized to improve MCAK’s functionality by promoting the release of the enzyme from detached tubulin subunits so that it can to undergo multiple rounds of action. However, overexpressed MCAK(Mono) generally outperforms MCAK(FL) as a microtubule depolymerizer in cells^{5,10,11}. This apparent contradiction led us to perform a thorough analysis of the role of dimerization in the absence of free tubulin in order to eliminate any effect of tubulin sequestration. This enabled us to specifically determine the effect that dimerization has on MCAK’s two most important activities on the microtubule: transport to microtubule ends and tubulin subunit removal.

We expressed and purified a GFP labeled mutant, MCAK(Mono) (“monomeric”, Fig. 1A) in which the N- and C-terminal dimerization domains had been deleted but the neck and motor domain is retained, similar to previously described monomeric mutants¹⁰. We determined k_b , the association rate, dissociation rate, diffusion coefficient, flux to microtubule end, and removal factor for MCAK(Mono). Unexpectedly, the monomeric mutant MCAK(Mono) exhibits a 15-fold higher association rate with the microtubule lattice than wild-type MCAK(FL) (Table 1). In addition, MCAK(Mono) exhibits a 2-fold increased dissociation rate (corresponding to shorter dwell times on the microtubule lattice) and a 20% increased

diffusion coefficient. However, the association rate provides the dominant influence, resulting in a net 11-fold higher flux to microtubule ends for MCAK(Mono). Thus, dimerization inhibits the delivery of MCAK to microtubule ends, primarily as a result of reduced lattice association rates.

Dimerization facilitates tubulin removal

MCAK(Mono) exhibits an 11-fold lower removal factor (Table 1) than the wild-type MCAK(FL). Thus, once the MCAK molecule arrives at the microtubule end, dimerization greatly enhances its ability to remove tubulin subunits. It might appear that in the case of dimerization, the benefits and detriments balance each other out, since the overall depolymerization efficacy as quantified by k_b reveals a nearly equal performance between MCAK(Mono) and MCAK(FL). However, for situations in which the delivery of MCAK to microtubule ends is enhanced by means other than lattice diffusion (such as recruitment by EB113 or direct anchoring to centromeres during mitosis) we would expect MCAK(FL) to depolymerize more effectively than MCAK(Mono). The reported enhanced ability of full-length dimeric MCAK to disengage from detached tubulin subunits¹² might further improve the effectiveness of the full-length enzyme in cells. Finally, the C-terminus of MCAK limits the tendency of the enzyme to hydrolyze ATP unproductively along the lattice¹⁴. In this way, the coupling of ATP hydrolysis to tubulin removal might be improved by domains outside of the core neck and motor at the expense of a slightly reduced lattice association rate^{12,14}.

In contrast to the comparable performance observed between MCAK(Mono) and MCAK(FL) at low concentrations, MCAK(Mono) substantially outperforms MCAK(FL) at saturating concentrations as quantified by a 15-fold increase in V_{max} . Importantly, this observation explains prior studies which showed MCAK(Mono) outperforming MCAK(FL) when each are overexpressed in cells^{5,10,11}. The cells in these assays almost certainly encounter saturating concentrations of MCAK, thus the data presented here would predict MCAK(Mono) to exhibit more effective depolymerization.

In order to verify the findings regarding the specific functionality of MCAK's positively charged neck and dimerization, we expressed and purified a third mutant protein MCAK(Mono-NN) (“monomeric, neutralized neck”, Fig. 1A) comprising a combination of the previous two mutations. We measured k_b , the association rate, dissociation rate, diffusion coefficient, flux to microtubule end, and removal factor for this mutant. As verification of the function of the positively charged neck, we expected to see the same trends when comparing MCAK(Mono-NN) to MCAK(Mono) as we observed when comparing MCAK(FL-NN) to MCAK(FL), namely a lower lattice association rate, a lower flux to the microtubule end, and a greater removal factor. As predicted, MCAK(Mono-NN) exhibits a roughly 22-fold lower lattice association rate, 18-fold lower flux to the microtubule end, and a 3-fold higher removal factor than MCAK(Mono). Likewise, as verification of the function of dimerization, we expected a comparison between MCAK(Mono-NN) and MCAK(FL-NN) to yield similar trends as we observed between MCAK(Mono) and MCAK(FL), namely a higher lattice association rate, a higher flux to the microtubule end, and a lower removal factor. Once again, the data matched our expectation

with MCAK(Mono-NN) exhibiting a 120-fold higher lattice association rate, 90-fold higher flux to the microtubule end, and a 13-fold lower removal factor than MCAK(FL-NN).

MCAK is likely to be processive but not cooperative

In addition to explaining functional contributions of MCAK's positively charged neck and dimeric structure, these data also provide several additional insights into the mechanism of MCAK operation. First, in addition to the Michaelis-Menten fit to the dose-response depolymerization data (Fig. 1B), we also fit the Hill equation to this data as a means to determine if MCAK exhibits cooperativity (Fig. S2). The Hill fit yields n values very close to 1 for wild-type MCAK(FL) and each of the three mutants (Fig. S2). This suggests that MCAK molecules do not act cooperatively, but rather as individual depolymerizing enzymes.

Second, as suggested above, the removal factor data (Table 1) is consistent with MCAK acting processively (i.e. undergoing multiple enzymatic cycles of tubulin subunit removal) at the microtubule end. Even more interesting, neutralization of the neck, while decreasing the on-rate and flux to the microtubule end may increase the processivity of the motor once it reaches the end. However, because the binding of one MCAK molecule at the microtubule end might have a net destabilization effect resulting in the simultaneous removal of several tubulin subunits, future single molecule analysis focused specifically on the action of MCAK molecules at the ends of microtubules will be required to establish whether or not MCAK acts processively.

An energy barrier must be negotiated to bind microtubule lattice

Plotting the microtubule lattice association rate versus dissociation rate for each of the four mutants, surprisingly reveals a positive trend (Fig. 3A). Stated explicitly, this means that a mutant such as MCAK(Mono) associates with the microtubule lattice more frequently than MCAK(FL), but is also more quick to fall off. Conversely, MCAK(FL-NN) very infrequently initiates an interaction with the microtubule lattice, but once it does, it is more likely to remain attached than wild type MCAK(FL) or any of the other mutants. In terms of the energy landscape, this implies that there is a barrier between the free-in-solution state and the lattice-bound state that can be raised or lowered with certain mutations to the molecule (Fig. 3B). A mutant such as MCAK(Mono) exhibits a low barrier and is therefore able to transition in either direction between the free-in-solution and lattice-bound states with high frequency (Fig. 3C). On the other hand MCAK(FL-NN) exhibits a tall barrier and thus transitions between the two states occur relatively infrequently (Fig. 3D).

DISCUSSION

Our data show that the function of the positively charged neck of MCAK is to negotiate an energy barrier that naturally impedes the direct association of the motor (and likely most microtubule associated proteins) with the microtubule lattice. The barrier also impedes dissociation from the microtubule once the protein is bound. Crossing the barrier is so important that a loss in tubulin removal efficiency is tolerated to catalyze it. The source of this barrier represents a fundamental question for future experiments in this matter. One

possible mechanism for generating such a barrier is a transitional restructuring of the hydration shell and associated ions that surround the MCAK molecule and the microtubule lattice. This type of water shell remodeling has been shown to occur in the non-specific association of DNA-binding proteins into the major and minor grooves of DNA¹⁵. DNA has a negatively charged surface, which polarizes and imparts additional structure to the water molecules in its immediate vicinity¹⁶. The arrival of a binding protein within this space remodels these hydration shells, which requires a high free energy during the transition¹⁷. Similar to DNA, microtubules carry a strong negative charge along their surface and thus we would expect to observe an analogous phenomenon. The potential significance of such a transitional state is that the high free energy required to cross the transitional barrier could serve to maintain attachment of the binding protein without the need for a strong binding motif. This would allow the binding protein, MCAK in this case, to diffuse somewhat freely along the microtubule yet not fall off, similar to the rapid 1-D diffusion observed with DNA binding proteins. Furthermore it offers a common mechanism to explain the ever-growing number of diverse proteins that have been shown to exhibit 1-D diffusion along microtubules ³⁰, including MCAK⁴, the Dam1 complex⁸, Eg5¹⁸, Myosin V¹⁹, CENP-E²⁰, and the Ndc80 complex²¹.

The highly non-specific and loose interaction of MCAK diffusing on microtubules is maintained not by direct binding groups but instead by entropic restructuring of the surrounding water and ions. Our study contradicts the idea that 1D diffusion of motors is a modified version of directed motility (ie randomly directed stepping²⁵). Published studies have shown that many non-motor molecules diffuse similarly on microtubules and MCAK does not “step” like a motile kinesin. Further support for this conclusion is our observation that the motor domain of MCAK is not necessary for diffusion because purified motorless MCAK diffuses avidly, similarly to wild-type motor (data not included). This study also contradicts that idea that diffusive behavior is conferred by a specific “diffusion domain”. The positively charged neck domain of MCAK has been previously implicated as a domain to electrostatically tether MCAK to microtubules during diffusion^{3,4}. We have shown, by removing the electrostatic charges in the neck without adversely affecting diffusion, that this is not the case.

The positively charged neck domain of MCAK is, however, an absolute requirement for the protein to exhibit microtubule depolymerization activity under physiological conditions⁵. In contrast to being a tether for diffusion, the neck catalyzes the association of motor to microtubules. The association constant for wild-type MCAK to microtubule ends is $96 \mu\text{M}^{-1}\text{s}^{-1}$, which is substantially higher than the typical range of on-rates for 3-D diffusion-limited protein associations ($0.5\text{--}8 \mu\text{M}^{-1}\text{s}^{-1}$)²⁷. Tubulin and actin polymerization, for example, fall within this range^{28,29}. The rate at which MCAK could find the microtubule end, $96 \mu\text{M}^{-1}\text{s}^{-1}$, is within 2 order of magnitude of the maximum theoretical association value of $7000 \mu\text{M}^{-1}\text{s}^{-1}$ predicted by the Einstein-Smoluchowski equation²⁶ for a situation without geometric constraints. Few association reactions approach this maximum rate (and most fall many orders of magnitude short) without facilitated diffusion afforded by either coulombic forces or reduction in dimensionality. We have parsed apart the relative contributions of these mechanisms by showing that the on-rate for MCAK (FL-NN) to microtubule ends ($0.67 \mu\text{M}^{-1}\text{s}^{-1}$) is $\sim 1/150$ of the on-rate for wild-type MCAK. Thus the

positively charged neck increases the on-rate to microtubule ends approximately 150-fold. This can be compared to the contribution of the reduction in dimensionality by diffusion or the “antenna effect”⁴. In this case, the on-rate of wild-type MCAK and MCAK (FL-NN) to the microtubule lattice is $3.6 \mu\text{M}^{-1}\text{s}^{-1}$ and $0.022 \mu\text{M}^{-1}\text{s}^{-1}$, respectively, while the on-rate to microtubule ends is, as stated above, $96 \mu\text{M}^{-1}\text{s}^{-1}$ and $0.67 \mu\text{M}^{-1}\text{s}^{-1}$. In both cases, diffusion along the lattice increases the on-rate to microtubule ends in MCAK and MCAK (FL-NN) by about 30-fold. This substantial enhancement of microtubule depolymerizing activity over the 3-D diffusion-limited on-rate has been demonstrated previously by Helenius et al.⁴. But we show here that 1-D diffusion is a constant for both wild-type MCAK and highly inefficient MCAK mutants. Collectively, then, the high on-rate of MCAK to microtubule ends is facilitated by a combination of on-rate catalysis (~150-fold) and reduction in dimensionality (~30-fold). Most importantly, we have shown that it is the on-rate, not the diffusion coefficient, that varies among mutant MCAK variants. This suggests that tuning the on-rate is the way that cells control microtubule depolymerase activity over an extremely broad kinetic range and is likely a major driving force during molecular evolution.

It is interesting that either the addition of positive charges to the neck or removal of dimerization domains increases both the association and the dissociation of MCAK with the microtubule lattice in parallel. A modest increase in the dissociation rate in parallel with the on-rate may be tolerated to traverse the energy barrier surrounding the microtubule. Or this property may help drive the delivery of MCAK to microtubule ends by enabling the molecule to hop from one diffusive site to another (Figure 3e) as in the dramatic case of monomeric MCAK. Without this capability, the motor may tend to repeatedly scan the same region on the microtubule resulting in a decrease in the flux of motor to the microtubule end.

The performance enhancement imparted by the positively charged neck comes with a tradeoff, in that the protein’s effectiveness at removing tubulin subunits is reduced. Conversely, dimerization affords MCAK an improved ability to remove tubulin subunits once at the microtubule end, but this improvement is countered by a reduction in microtubule lattice association rate. Some of the reduced performance in lattice binding could potentially be offset *in vivo* by direct recruitment of MCAK to microtubule ends at centromeres or by the microtubule tip-tracking protein EB113. Regardless, catalysis of the association of MCAK with microtubules is the most important parameter controlling the efficiency of MCAK’s depolymerizing activity. The structures that catalyze microtubule association constitute superb candidate domains for cellular regulation of MCAK and, most likely, any protein that diffuses on microtubules.

METHODS

Protein expression

We purified Wild-type and mutant EGFP labeled MCAK proteins as described¹⁰, except that the pFastBac1 plasmid (Invitrogen) was used to construct recombinant baculoviruses. MCAK(FL-NN) includes point mutations to positively charged amino acid residues in the neck as described⁵. See Figure 1 for diagrams of the MCAK mutants. Concentrations of monomeric mutants (MCAK(Mono) and MCAK(Mono-NN)) are reported as concentrations of active ATP-binding sites. For dimeric mutants (MCAK(FL) and MCAK(FL-NN)) the

concentration of active ATP-binding sites was divided by 2 to provide a true molecular concentration.

Microtubules

We purified tubulin from bovine brains and fluorescently labeled tubulin with NHS-ester Cy5 dye (Amersham) per standard techniques^{22,23}. GMPCPP stabilized microtubules were grown at 37° C from a 30:1 mixture of unlabeled and Cy5-labeled tubulin. Taxol stabilized microtubules were grown at 37° C from a 300:1 mixture of unlabeled and Cy5-labeled tubulin in BRB80 + 5% DMSO, 5 mM MgCl₂, and 2 mM GTP and immediately diluted into BRB80 + 10 μM taxol (Sigma). Microtubules were pelleted to remove unpolymerized tubulin and then resuspended in BRB80 + μ10 M taxol.

TIRF Configuration

We collected TIRF data using a Nikon TE2000-S inverted microscope with a custom two-color TIRF illumination system. The TIRF configuration was objective-based using a 100X, 1.49 NA Nikon objective. GFP was excited with a 473 nm laser (LaserPath Technologies) and Cy5 was excited with a 637 nm laser (Blue Sky Research). We recorded simultaneous red and green images on an Andor Ixon DV887ECS-BV back-illuminated EMCCD.

Depolymerization Assay Conditions

After initially rinsing with ddH₂O, we filled flow chambers constructed with double-stick tape with BRB80 + 70 mM KCl, 1 mg/mL κ-casein (sigma), and ~10 g/mL G234A rigor-kinesin 24. After incubating for ~5 min, flow chambers were rinsed thoroughly with BRB80 + 70 mM KCl and 1 mg/mL κ-casein.

For depolymerization assays, GMPCPP stabilized microtubules were drawn into the chamber and allowed to link up to the surface-bound rigor-kinesin. After incubating for ~5 min, the chamber was rinsed and assay buffer containing MCAK(FL) (or one of the three mutant forms) was then drawn into the chamber. Assay buffer was composed of BRB80 + 70 mM KCl, 1 mg/mL κ-casein, 2 mM ATP, 200 μg/ml glucose oxidase, 35 μg/ml catalase, 25 mM glucose and 5 mM DTT. Images were recorded at 1 frame per second.

For single molecule assays, the flow chambers were prepared in the same manner as for depolymerization assays (described above), except taxol stabilized microtubules were used and images were recorded at 10 frames per second.

Photobleach measurements

For single molecule photobleach measurements, the flow chambers were prepared identically except nucleotides were omitted resulting in MCAK molecules binding the microtubule lattice in a “rigor”-like fashion such that the photobleach rates can be measured without dissociation of the molecule. Figure S1 provides four examples of the characteristic two-step photobleach pattern observed for dimeric EGFP labeled MCAK(FL). The average photobleach rate for EGFP under the conditions of the single molecule experiments was measured using MCAK(Mono), which being a monomer, exhibits one-step photobleach

events. This rate was used to correct the measurement of the average dwell time for photobleaching effects (see analysis section below)

Analysis

Movies were imported into Igor Pro 6.0 (Wavemetrics) for analysis. Custom routines written within the Igor programming environment were used to analyze both depolymerization rates and single molecule kinetics. An edge finder routine was applied to the microtubule kymographs at each time point to calculate the instantaneous length of the microtubule throughout the movie. The depolymerization rate for each microtubule was measured by fitting a regression line to the length vs. time curve, thus this measurement reflects the combined depolymerization of both microtubule ends. Each data point shown in the dose-response curve (Fig. 1) represents an average of between 20 and 50 microtubules imaged from at least 2 but usually 3 or more separate flow cells. An average baseline depolymerization rate of 0.005 $\mu\text{m}/\text{min}$ was calculated from microtubules from 5 separate flow cells prepared as described above, but lacking MCAK. This baseline rate was subtracted from each of the individual depolymerization rate measurements to obtain the final dose-response data. Data was fit to both the Michaelis-Menten equation (Fig. 1) to yield the parameters V_{max} and $K_{1/2}$ and the Hill equation (Fig. S2) to yield the parameters V_{max} , $K_{1/2}$, and n .

Single molecule landing events were tracked by fitting a two-dimensional gaussian function frame-by-frame to every bright spot that landed on the microtubule lattice and dwelled there for 0.3 seconds (3 frames) or longer. Displacements were measured longitudinally to the microtubule axis and mean square displacements were calculated at 0.1 sec increments. Diffusion coefficients were calculated as described⁴. The fact that the diffusion coefficient measured here is lower than that of previously published study of MCAK⁴ is most likely due to the differences in the source of tubulin (species and post-translational modifications) for the microtubules used in the assays and to differences, in the ionic strength between the two studies. The diffusion coefficients measured in this study are fully consistent with others measured using the same microtubules⁸. Dissociation rates were calculated by fitting a single exponential to each histogram of dwell times (Fig. 2) and taking the reciprocal of the time constant, τ_{DIS} . This measurement was corrected for the effects of photobleaching as described⁴. The total number of events was estimated by integrating the exponential fit to the dwell time histogram from 0 to ∞ . This is more accurate than simply counting up events because it accounts for the “missing events” that have a shorter dwell time than the threshold 0.3 seconds. The calculation of the total number of events was then divided by the total time, microtubule length, and concentration to achieve a measurement of the association rate onto the microtubule lattice. These measured kinetic parameters were averaged from thousands of events from at least 4 separate flow cells (per mutant) imaged on different days.

The “removal factor” was calculated by first converting the catalytic efficiency (k_b) to a measure of tubulin subunits removed from each microtubule end per second per [nM]. A conversion factor of 1750 tubulin subunits per micron of microtubule length was used and the result was subsequently divided by 2 to account for the fact that depolymerization rates were a measure of the combined shortening rates of both microtubule ends. Finally, this

number was divided by the flux of MCAK to each microtubule end (J_0/C_m) to yield a measure of the average number of tubulin subunits removed for each MCAK end-binding event.

Supplementary Material

Refer to Web version on PubMed Central for supplementary material.

Acknowledgements

The authors acknowledge support from the National Institutes of Health (GM069429) and from the National Science Foundation (IGERT traineeship to J. C.).

References Cited

1. Wordeman L, Wagenbach M, von Dassow G. MCAK facilitates chromosome movement by promoting kinetochore microtubule turnover. *The Journal of cell biology*. 2007; 179:869–879. [PubMed: 18039936]
2. Desai A, Verma S, Mitchison TJ, Walczak CE. Kin I kinesins are microtubule-destabilizing enzymes. *Cell*. 1999; 96:69–78. [PubMed: 9989498]
3. Hunter AW, et al. The kinesin-related protein MCAK is a microtubule depolymerase that forms an ATP-hydrolyzing complex at microtubule ends. *Molecular cell*. 2003; 11:445–457. [PubMed: 12620232]
4. Helenius J, Brouhard G, Kalaidzidis Y, Diez S, Howard J. The depolymerizing kinesin MCAK uses lattice diffusion to rapidly target microtubule ends. *Nature*. 2006; 441:115–119. [PubMed: 16672973]
5. Ovechkina Y, Wagenbach M, Wordeman L. K-loop insertion restores microtubule depolymerizing activity of a "neckless" MCAK mutant. *The Journal of cell biology*. 2002; 159:557–562. [PubMed: 12446739]
6. Ogawa T, Nitta R, Okada Y, Hirokawa N. A common mechanism for microtubule destabilizers-M type kinesins stabilize curling of the protofilament using the class-specific neck and loops. *Cell*. 2004; 116:591–602. [PubMed: 14980225]
7. Moores CA, et al. The role of the kinesin-13 neck in microtubule depolymerization. *Cell cycle (Georgetown, Tex)*. 2006; 5:1812–1815.
8. Gestaut DR, et al. Phosphoregulation and depolymerization-driven movement of the Dam1 complex do not require ring formation. *Nature cell biology*. 2008; 10:407–414. [PubMed: 18364702]
9. Thorn KS, Ubersax JA, Vale RD. Engineering the processive run length of the kinesin motor. *The Journal of cell biology*. 2000; 151:1093–1100. [PubMed: 11086010]
10. Maney T, Wagenbach M, Wordeman L. Molecular dissection of the microtubule depolymerizing activity of mitotic centromere-associated kinesin. *The Journal of biological chemistry*. 2001; 276:34753–34758. [PubMed: 11466324]
11. Newton CN, Wagenbach M, Ovechkina Y, Wordeman L, Wilson L. MCAK, a Kin I kinesin, increases the catastrophe frequency of steady-state HeLa cell microtubules in an ATP-dependent manner in vitro. *FEBS letters*. 2004; 572:80–84. [PubMed: 15304328]
12. Hertzler KM, et al. Full-length dimeric MCAK is a more efficient microtubule depolymerase than minimal domain monomeric MCAK. *Molecular biology of the cell*. 2006; 17:700–710. [PubMed: 16291860]
13. Lee T, Langford KJ, Askham JM, Bruning-Richardson A, Morrison EE. MCAK associates with EB1. *Oncogene*. 2008; 27:2494–2500. [PubMed: 17968321]
14. Moore A, Wordeman L. C-terminus of mitotic centromere-associated kinesin (MCAK) inhibits its lattice-stimulated ATPase activity. *The Biochemical journal*. 2004; 383:227–235. [PubMed: 15250824]

15. Privalov PL, et al. What drives proteins into the major or minor grooves of DNA? *Journal of molecular biology*. 2007; 365:1–9. [PubMed: 17055530]
16. Kopka ML, Fratini AV, Drew HR, Dickerson RE. Ordered water structure around a B-DNA dodecamer. A quantitative study. *Journal of molecular biology*. 1983; 163:129–146. [PubMed: 6834428]
17. Levy Y, Onuchic JN. Water mediation in protein folding and molecular recognition. *Annual review of biophysics and biomolecular structure*. 2006; 35:389–415.
18. Kapitein LC, et al. The bipolar mitotic kinesin Eg5 moves on both microtubules that it crosslinks. *Nature*. 2005; 435:114–118. [PubMed: 15875026]
19. Ali MY, et al. Myosin Va maneuvers through actin intersections and diffuses along microtubules. *Proceedings of the National Academy of Sciences of the United States of America*. 2007; 104:4332–4336. [PubMed: 17360524]
20. Kim Y, Heuser JE, Waterman CM, Cleveland DW. CENP-E combines a slow, processive motor and a flexible coiled coil to produce an essential motile kinetochore tether. *The Journal of cell biology*. 2008; 181:411–419. [PubMed: 18443223]
21. Powers AF, et al. The Ndc80 kinetochore complex uses biased diffusion to couple chromosomes to dynamic microtubule tips. *Cell*. 2009
22. Hyman A, et al. Preparation of modified tubulins. *Methods in enzymology*. 1991; 196:478–485. [PubMed: 2034137]
23. Mickey B, Howard J. Rigidity of microtubules is increased by stabilizing agents. *The Journal of cell biology*. 1995; 130:909–917. [PubMed: 7642706]
24. Rice S, et al. A structural change in the kinesin motor protein that drives motility. *Nature*. 1999; 402:778–784. [PubMed: 10617199]
25. Bormuth V, et al. Protein friction limits diffusive and directed movements of kinesin motors on microtubules. *Science*. 2009; 325:870–873. [PubMed: 19679813]
26. Smoluchowski S. Versuch einer mathematischen Theorie der koagulationskinetik kolloider Lösungen. *Zeitschrift für physikalische chemie*. 1918; 92:129–168.
27. Northrup SH, Erickson HP. Kinetics of protein-protein association explained by Brownian dynamics computer simulation. *Proceedings of the national academy of sciences USA*. 1992; 89:3338–3342.
28. Pollard TD, Cooper JA. Actin and actin-binding proteins. A critical evaluation of mechanisms and functions. *Annual review of biochemistry*. 1986; 55:987–1035.
29. Caplow M, et al. The free energy for hydrolysis of a microtubule-bound nucleotide triphosphate is near zero: all of the free energy for hydrolysis is stored in the microtubule lattice. *Journal of cell biology*. 1994; 127:779–778. [PubMed: 7962059]
30. Cooper JR, Wordeman L. The diffusive interaction of microtubule binding proteins. *Current Opinion in Cell Biology*. 2009; 21:68–73. [PubMed: 19185482]

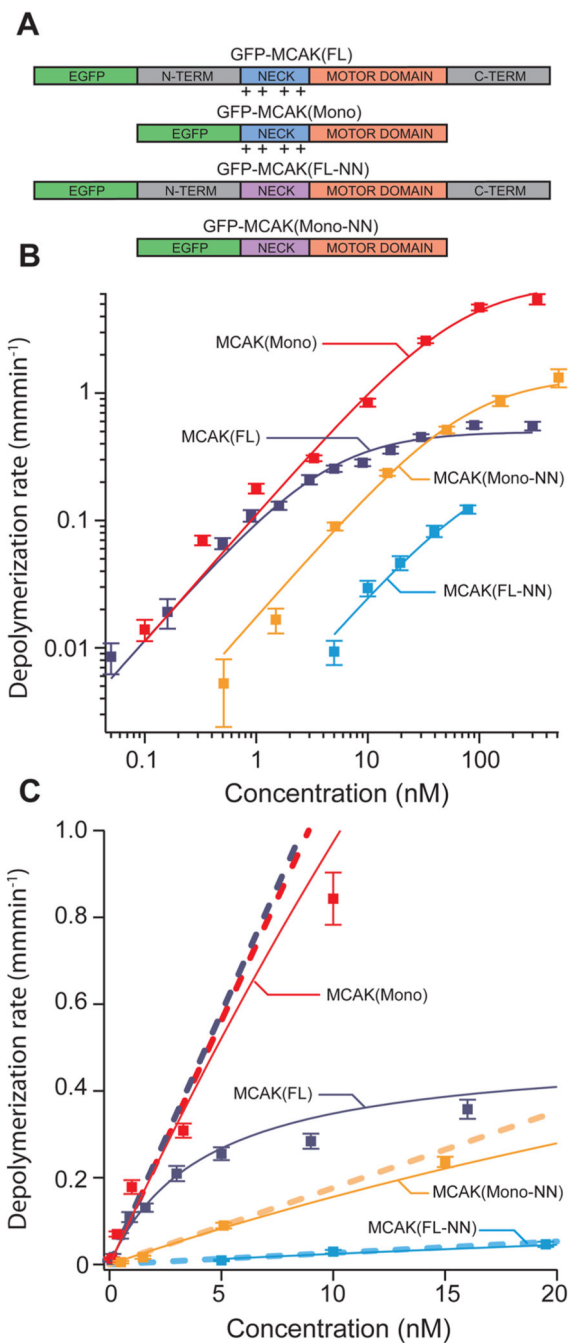


Figure 1. MCAK mutants exhibit shifted microtubule depolymerization dose-response curves (A) Diagram of mutated MCAK regions. Wild-type MCAK(FL) consists of the motor domain (orange), a positively charged neck region (blue), and n-terminal and c-terminal domains (grey). MCAK(Mono) is missing both the n-terminal and c-terminal domains, which renders the protein unable to dimerize. MCAK(FL-NN) has several of the positively charged residues in the neck region replaced with neutral alanine residues (purple). MCAK(Mono-NN) combines these mutations. (B) Log-scale plot of average microtubule depolymerization rate vs. MCAK concentration. Data from each of the four MCAK mutants

is shown with a Michaelis-Menten fit curve. Error bars reflect s.e.m. values. (C) Linear-scale plot of the same data presented in panel B. The slope of the asymptote (dashed line) associated with each fit curve measures catalytic efficiency (k_b). Note: some of the data points at high concentration and/or depolymerization rate land off the scale of the linear plot but are included in the log-scale plot (panel B).

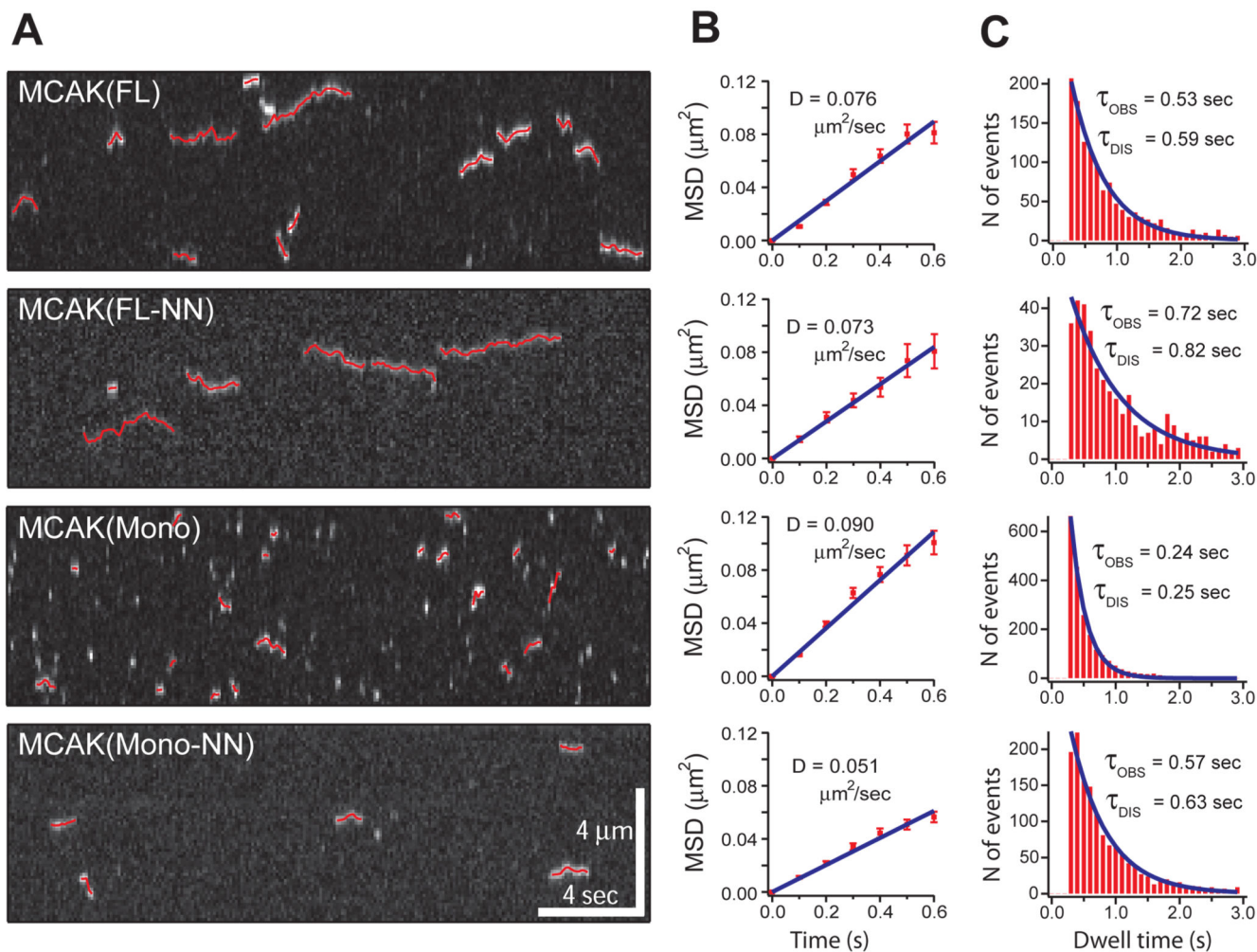


Figure 2. Diffusive behavior of single MCAK molecules and mutants

(A) Kymographs demonstrate single molecule diffusion of MCAK(FL) and mutant MCAK proteins. All four of the tested MCAK proteins can bind to and diffuse along the microtubule lattice, although with radically different association rates (k_{ON}) and dissociation rates (k_{OFF}). 2-dimensional Gaussian fit tracks of the moving spots are overlaid in red. (B) The mean square displacements for each of the four tested MCAK proteins are shown plotted at 0.1 second time intervals. Diffusion coefficients (D) are calculated as the slope/2 of the fit line. (C) Distributions of event dwell times for each of the four tested MCAK proteins shown with a single exponential fit curve. τ_{OBS} reflects the observed average event duration. τ_{DIS} has been corrected for photobleaching and is thus the average time prior to event dissociation.

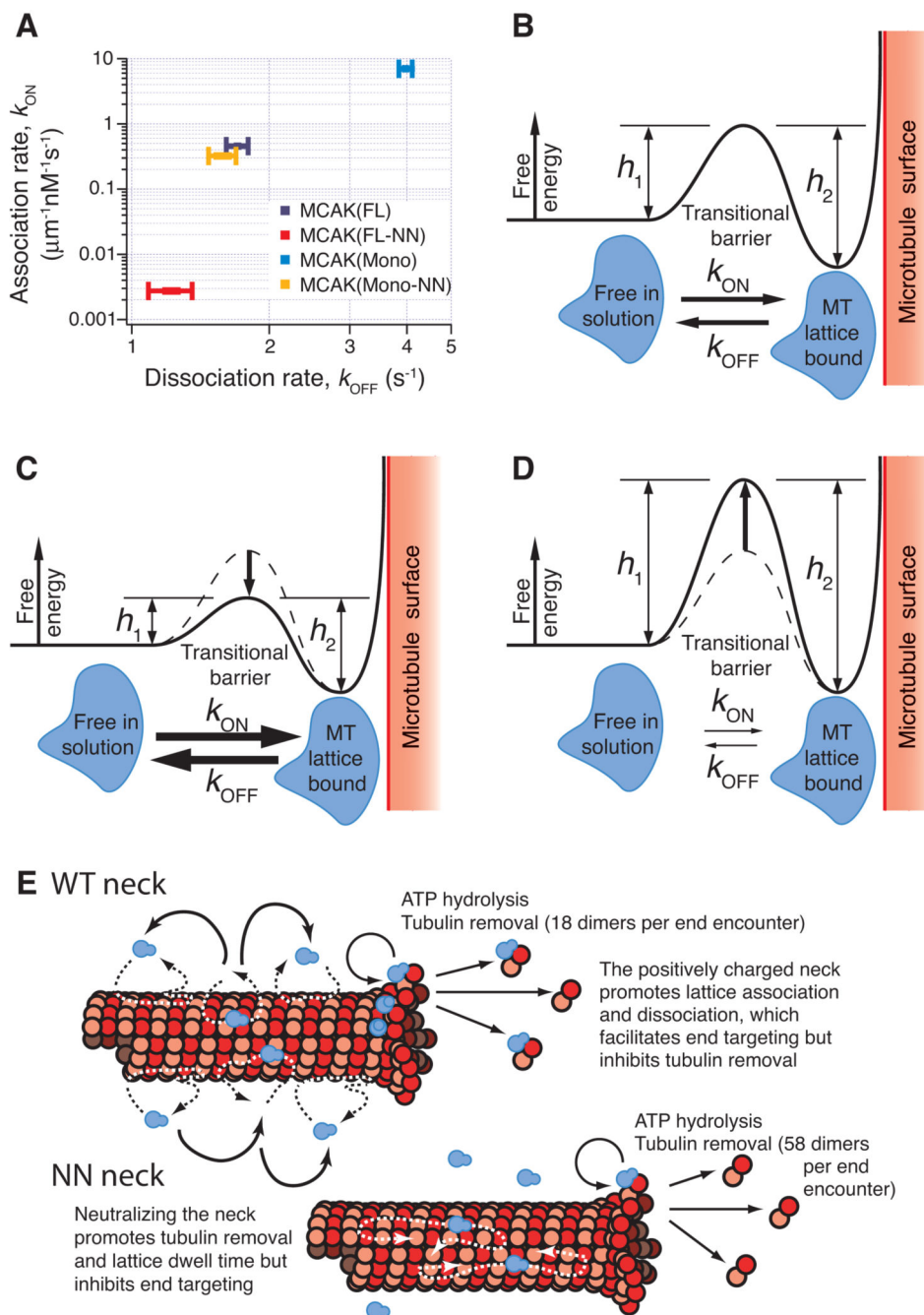


Figure 3. A positive correlation between k_{ON} and k_{OFF} is consistent with an energy landscape model for diffusive binding

(A) Association rates (k_{ON}) for MCAK(FL) and each of the three tested MCAK mutants plotted against the respective dissociation rates (k_{OFF}). This plot demonstrates a positive relationship between k_{ON} and k_{OFF} , which can be explained by a transitional barrier of variable height as shown in (B). The MCAK molecule (blue) must pass through the high-energy transitional state in order to switch between the two stable low energy states: free-in-solution or microtubule-bound. k_{ON} represents the transition from free-in-solution to microtubule-bound and is inversely dependent upon the height h_1 . Alternately, k_{OFF}

represents the transition from microtubule-bound to free-in-solution and is inversely dependent upon the height h_2 . (C) The data indicates that MCAK(Mono) has a reduced barrier height in comparison to MCAK(FL), which explains the observed increases in both k_{ON} and k_{OFF} . (D) Conversely, MCAK(FL-NN) has an increased barrier height, indicated by the observed decreases in both k_{ON} and k_{OFF} . (E) Model illustrating the parameters that affect the flux of motors to the microtubule end and the removal of tubulin from the microtubule end.

Author Manuscript

Author Manuscript

Author Manuscript

Author Manuscript

Table 1
Quantification of key factors controlling the depolymerase activity of MCAK

Key functional parameters of MCAK(FL) and three mutant MCAK proteins. The catalytic efficiency (k_b) is calculated from a Michaelis-Menten fit to the depolymerization rate dose-response data (Fig. 1). Diffusion coefficients (D) were measured from a plot of mean square displacement vs. time (Fig. 2B) and reflect only the diffusion parallel to the axis of the microtubule (the perpendicular component is very close to zero). Association rates (k_{ON}) and dissociation rates (k_{OFF}) were calculated from the dwell time distributions of landing events (Fig. 2C). The flux of MCAK molecules arriving at each microtubule end via lattice diffusion (J_0/C_m), was calculated from D, k_{ON} , and k_{OFF} by the flux equation noted in the text. The removal factor is an estimate of the number of tubulin subunits removed on average for a single MCAK end-binding event (see full methods).

	Catalytic Efficiency (k_b)	Diffusion Coefficient (D)	Association Rate (k_{ON})	Dissociation Rate (k_{OFF})	Flux to Microtubule End (J_0/C_m)	Removal Factor
	($\mu\text{m}/\text{min}$) nM	($\mu\text{m}^2/\text{sec}$)	(events/sec) $\mu\text{m}\cdot\text{nM}$	(events/sec)	(events/sec) nM	
MCAK(FL)	0.116 ± 0.011	0.076 ± 0.003	0.456 ± 0.008	1.70 ± 0.09	0.096 ± 0.007	18 ± 2
MCAK(FL-NN)	0.0026 ± 0.0012	0.073 ± 0.001	0.00274 ± 0.00013	1.22 ± 0.13	0.00067 ± 0.00008	58 ± 27
MCAK(Mono)	0.112 ± 0.013	0.090 ± 0.003	6.99 ± 0.09	3.98 ± 0.13	1.05 ± 0.05	1.6 ± 0.2
MCAK(Mono-NN)	0.018 ± 0.003	0.051 ± 0.002	0.323 ± 0.015	1.58 ± 0.11	0.058 ± 0.005	4.5 ± 0.9